Journal of the European Ceramic Society 20 (2000) 1521–1525

Elastic degradation of an advanced silicon nitride during tensile creep

Akira Okada [a,*], Frantisek Lofaj [b]

[a] *Japan Fine Ceramics Center, Nagoya 456, Japan*
[b] *Institute of Materials Research of the Slovak Academy of Sciences, 043 53 Kosice, Slovakia*

Received 5 July 1999; received in revised form 25 October 1999; accepted 4 November 1999

Abstract

Tensile creep tests were conducted on an advanced silicon nitride at 1400°C in air. During the creep tests, an intermediate layer with precipitates was formed under the subsurface oxidation layer. Microstructure observation revealed the presence of numerous microcracks, which developed perpendicular to the tensile stress axis. The local elastic properties of the cross-section of crept specimens were examined by the micro-indentation technique and elastic degradation was found in the subsurface layers. While the creep curves exhibit transient and steady-state-like stages, the creep rate gradually increases in the steady-state-like stage. The origin of this slightly accelerated stage is discussed.

Keywords: Creep; Elastic modulus; Indentation; Oxidation; Si_3N_4

1. Introduction

Silicon nitride has been successfully used in mechanical components such as turbocharger rotors, glow plugs, high-speed bearings and cutting tools.[1,2] The excellent mechanical properties of silicon nitride at elevated temperatures have led to the expectation of its being used in ceramic gas turbines, which enable improved thermal efficiencies to be achieved by operating at high temperature.[3,4] Careful design and processing are, however, required for such mechanical applications due to the brittle nature of ceramic materials. Designing ceramic components to reduce the maximum stress and use of careful manufacturing processes to minimize the dimension of flaws are, therefore, essential to avoid unexpected failure. Furthermore, developing an accurate lifetime prediction method is important for assuring reliability in practical applications. It is noteworthy that the lifetime of ceramics is generally governed by the strength degradation, while in some cases the lifetime is controlled by the dimensional change occurring in the materials.

The lifetime under loading at high temperatures can be controlled by several degradation mechanisms. Subcritical crack growth from a pre-existing flaw is a well-known mechanism for strength degradation in ceramics. The estimation of the residual strength is, however, difficult due to the lack of warning signs such as plastic deformation prior to final failure. Proof testing is, therefore, widely applied to assure the lifetime and reliability.[5,6] Creep rupture is another mechanism of reducing the residual strength. Both of these mechanisms are similar to each other since creep rupture in ceramics often occurs in a region of very small deformation. However, it should be noted that creep rupture results from cavity formation followed by coalescence of the cavities. while failure resulting from subcritical crack growth originates from the largest pre-existing flaw. In advanced silicon nitrides, the subcritical crack growth mechanism is generally dominant at temperatures below approximately 1100°C under high stresses corresponding to a lifetime up to 1000 h.[7] Accordingly, creep rupture is predominant at higher temperatures under lower stresses, where the corresponding lifetime is considerably longer than that resulting from the subcritical crack growth mechanism. A fracture mechanism map for silicon nitride SN88 (NGK Insulators Ltd. Nagoya, Japan), for example, indicates that creep

* Corresponding author. Tel.: +81-52-871-3500; fax: +81-52-87-3599.
E-mail address: okada@jfcc.or.jp (A. Okada).

0955-2219/00/$ - see front matter
PII: S0955-2219(00)00031-5

rupture at a temperature of 1070°C is predominant for lifetimes exceeding 1000 h whereas the subcritical crack growth mechanism is predominant for lifetimes less than 1000 h.[8] In the case of large creep deformation, deformation exceeding an allowable limit determines the lifetime of use. The third degradation mechanism is that due to severe flaw generation such as oxidation and corrosion. In particular, oxidation of non-oxide ceramics governs the lifetime in cases where degradation of the residual strength occurs intensively. Another mechanism due to oxidation which is responsible for limitation of use is the significant dimensional changes that result from the formation of oxide layers. Additionally, in the case of rotating parts such as gas turbine rotors, impact damage caused by small fragments migrating into the rotating parts may lead to a reduction in strength.

In actual high temperature tests, oxidation usually occurs in non-oxide ceramics and may affect the measured properties. In the present study, tensile creep tests of an advanced silicon nitride were conducted and the oxidation effect on the creep behavior was explored in terms of oxidation-induced degradation occurring in the subsurface layer.

2. Experimental procedure

A gas pressure sintered silicon nitride (developmental grade: ST-1, supplied from NGK Spark Plugs Co., Ltd., Nagoya, Japan) was used in the present study. The microstructure of the material exhibits a typical bimodal grain size distribution, consisting of a small amount of large grains with length up to 5 μm dispersed in a matrix of small grains of 0.3–0.5 μm in lengths and 0.2 μm in diameter. The presence of ytterbium and aluminum in secondary phases was identified with a scanning electron microscope equipped with an energy dispersion X-ray analyzer (Model S-800, Hitachi, Japan). X-ray diffraction (PW 1752/00, Philips, The Netherlands) revealed that the major phase is β-Si_3N_4 and additional minor phases are α-Si_3N_4 and $Yb_2Si_7O_7$. The material has a bulk density of 3.37 Mg/m^3, the fracture toughness determined by the single-edge-precracked beam method is 5.6 $MPa.m^{1/2}$ and Young's modulus at room temperature determined by the ultrasonic pulse method was 317 GPa. The material has a four-point flexural strength of 1085 MPa at room temperature and the strength at 1400°C is 480 MPa.[9]

Dog-bone shaped specimens with a rectangular cross-section of 4×2.5 mm and gauge length of 20 mm were used for the tensile creep tests. Creep machines with dead weight loading (HTT-300, Toshin Co., Ltd., Tokyo, Japan) were employed in the present study and the specimens were fixed in the hot grips using four pins made of silicon carbide. The bending moments on the specimens were minimized by adjusting the load train and controlled using four strain gauges glued on each surface of the specimen. Creep strains were measured with two linear variable differential transducers (LVDT) outside the furnaces and in some cases with an optical extensometer (Model 4100, Zimmer, Germany) monitoring the position of flags integrated in the specimens.

The effective elastic modulus in local areas was determined by the Vickers indentation technique using a dynamic microhardness tester (Fischerscope. H100VP-HCU, Helmut Fisher GmbH, Germany). In this equipment, the values of the elastic modulus $E/(1-\nu^2)$, where E is Young's modulus and ν is Poisson's ratio, are automatically calculated from the slope of an unloading curve describing the relation between load and indentation depth. In the actual measurements, a Vickers indentor was loaded on the polished cross-sections of the crept specimen in 60 steps with dwell times of one second at each step, up to the maximum load of 300 mN. The same conditions were used during unloading. The cross-sections were cut perpendicular and parallel to the direction of the applied stress. It is noteworthy that the measured values of elastic modulus represent the averaged properties of the material because the diagonal length of the impression is about 10 μm, which is much greater than the dimension of the matrix grains. The details of the experimental procedure are described elsewhere.[9–11]

3. Results and discussion

Fig. 1a shows a scanning electron micrograph of the silicon nitride, the creep test of which was conducted at 1400°C under a stress of 70 MPa, and the rupture occurred after 84.8 h. The micrograph indicates the cross section perpendicular to the stress axis. Three regions with different brightness are seen. The oxidized layer, which looks white, is formed on the surface and its thickness is approximately 40 μm. The intermediate layer, which is dark gray with white precipitates, is formed under the oxidized layer and its thickness is approximately 400 μm. It is noteworthy that the concentration of white precipitates in the intermediate layer is low in the area near the surface. The bulk material with light gray color is seen under the intermediate layer. Chemical analysis using an EDAX revealed a high concentration of ytterbium and oxygen in the white precipitates in the intermediate layer and in the surface oxidized layer. This suggests that ytterbium diffuses toward the surface in the outer part of the intermediate layer. Fig. 1b shows another scanning electron micrograph of the cross section parallel to the stress axis. This sample was tested at 1400°C under a stress of 70 MPa and the rupture occurred after 36.5 h. During the test, the oxidation layer of approximately 10 μm and the

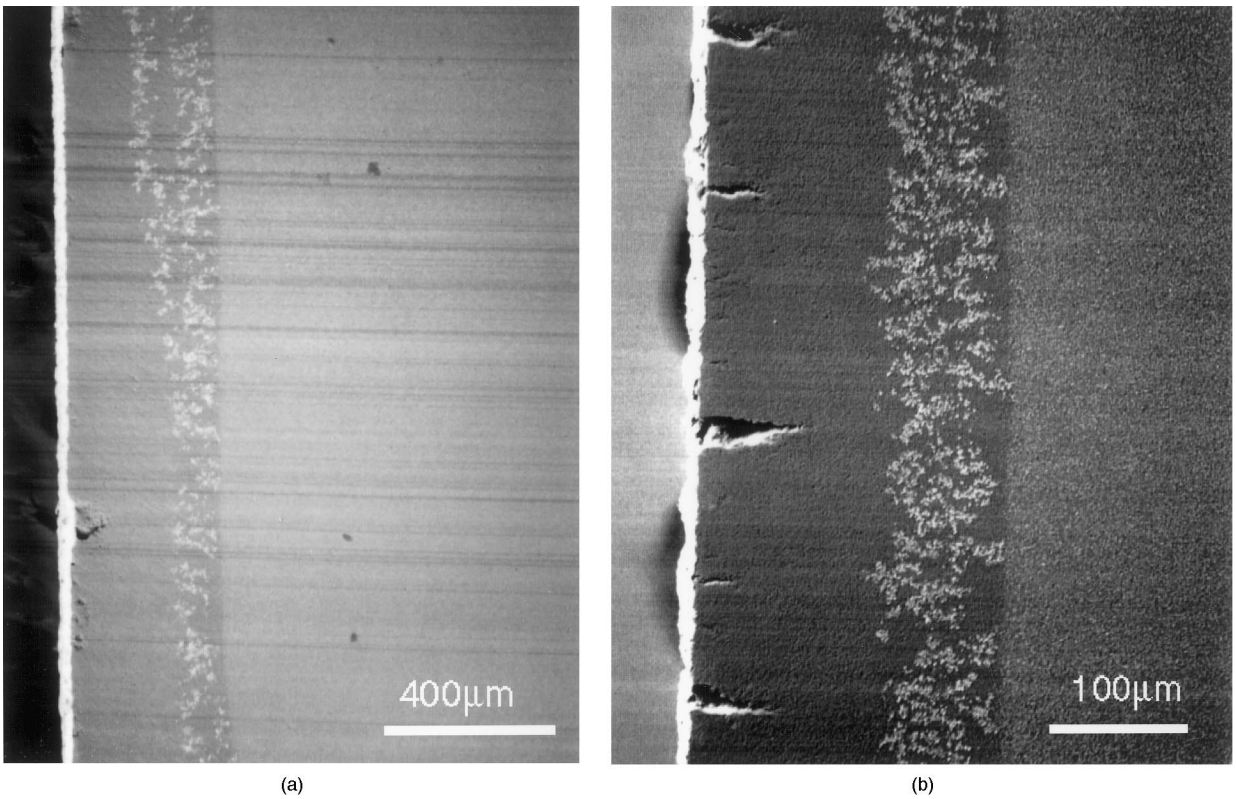

Fig. 1. Scanning electron micrographs of a cross-section of crept silicon nitride. (a) Perpendicular to the tensile stress. The test was conducted at 1400°C for 84.8 h under a stress of 70 MPa. (b) Parallel to the tensile stress, crack-like voids are visible. The test was conducted at 1400°C for 36.5 h under a stress of 70 MPa.

intermediate layer of approximately 220 μm thickness were formed. Surface cracks of several tens of microns are seen to be developed perpendicular to the direction of the tensile stress. This implies that the mechanical strength in the intermediate layer is lower than that of the core material. Note that the crack opening displacement is much greater than the several tenths of microns predicted from linear elastic fracture mechanics and that the crack tips are arrested in the intermediate layer. The stress concentration at the crack tip seems to be relaxed by the occurrence of the localized plastic deformation. It is noteworthy that the numerous cracks are observed only in the region near the surface and they are arrested. This implies that the final failure predominantly occurs not by oxidative degradation during creep but by creep rupture. In addition, two micrographs were taken from crept specimens conducted under the same test conditions. The reason for the different lifetimes between 36.5 and 84.8 h is unclear but this result seems to indicate the relatively large scatter in time-to-failure of creep rupture.

Fig. 2 shows the local distribution of the effective Young's modulus, $E/(1-\nu^2)$, in the cross-section area of the crept specimen, which was tested at 1400°C under a stress of 70 MPa for 84.8 h. In the case of a stress free part that was taken from an integrated flag of the specimen, the values of the modulus in the core zone at

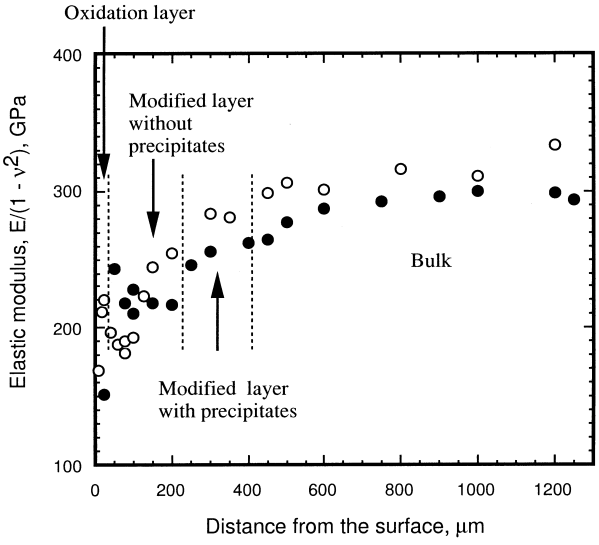

Fig. 2. Elastic modulus $E/(1-\nu^2)$ in the cross-section of the crept silicon nitride. The creep test was conducted at 1400°C for 84.8 h under a stress of 70 MPa. ●: Cross-section perpendicular to the tensile axis; ○: cross-section of a stress free part, taken from one of the integrated flags.

a distance of more than 500 μm from the surface are approximately 310 GPa. This is very close to the value of 317 GPa in the initial material. In contrast, the modulus in the intermediate layer of approximately 260

GPa is lower and the elastic modulus of the surface oxide layers is only about 200 GPa. The average value in the intermediate layer is about 16% lower than that in the bulk. The values of modulus for the cross-section perpendicular to the stress axis exhibit a similar trend but the modulus values are slightly lower. This is because the tensile stress produces cavities that contribute to lowering of the modulus. Since the elastic modulus is high in the core of the specimens, the stresses in the core are higher than the nominal ones. Furthermore, the actual stress in the core may be much higher because of intensive cracking of the surface layer, which is unable to support the load.

Fig. 3 shows typical creep curves obtained at 1400°C under stresses of 70 and 50 MPa. Transient creep regions are seen in the initial 20 h in both cases and the steady-state-like creep regions follow. It is noteworthy that the strain rates in the steady state region gradually increase with time, suggesting slightly accelerated creep deformation. The strain rates in the steady-state regions, indicated by solid lines in Fig.3a and b, are approximately $6\sim8\times10^{-7}$ and $2.5\sim3.7\times10^{-7}$ s^{-1}, respectively. But they increase linearly with time, and the increasing rates of the strain rates for 70 and 50 MPa are 9.7×10^{-13} and 2.4×10^{-13} s^{-2} respectively. This accelerated creep is probably caused by the increase in the effective stress in the load-bearing core of the specimens, as a result of reduction in elastic modulus and crack generation in the intermediate layers. Another possible mechanism is generation of cavities during creep deformation.[12–16] However, it was reported that generation of cavities increases the creep rate through the higher stress component of creep deformation in higher stress regions while gradual increases in creep rates have

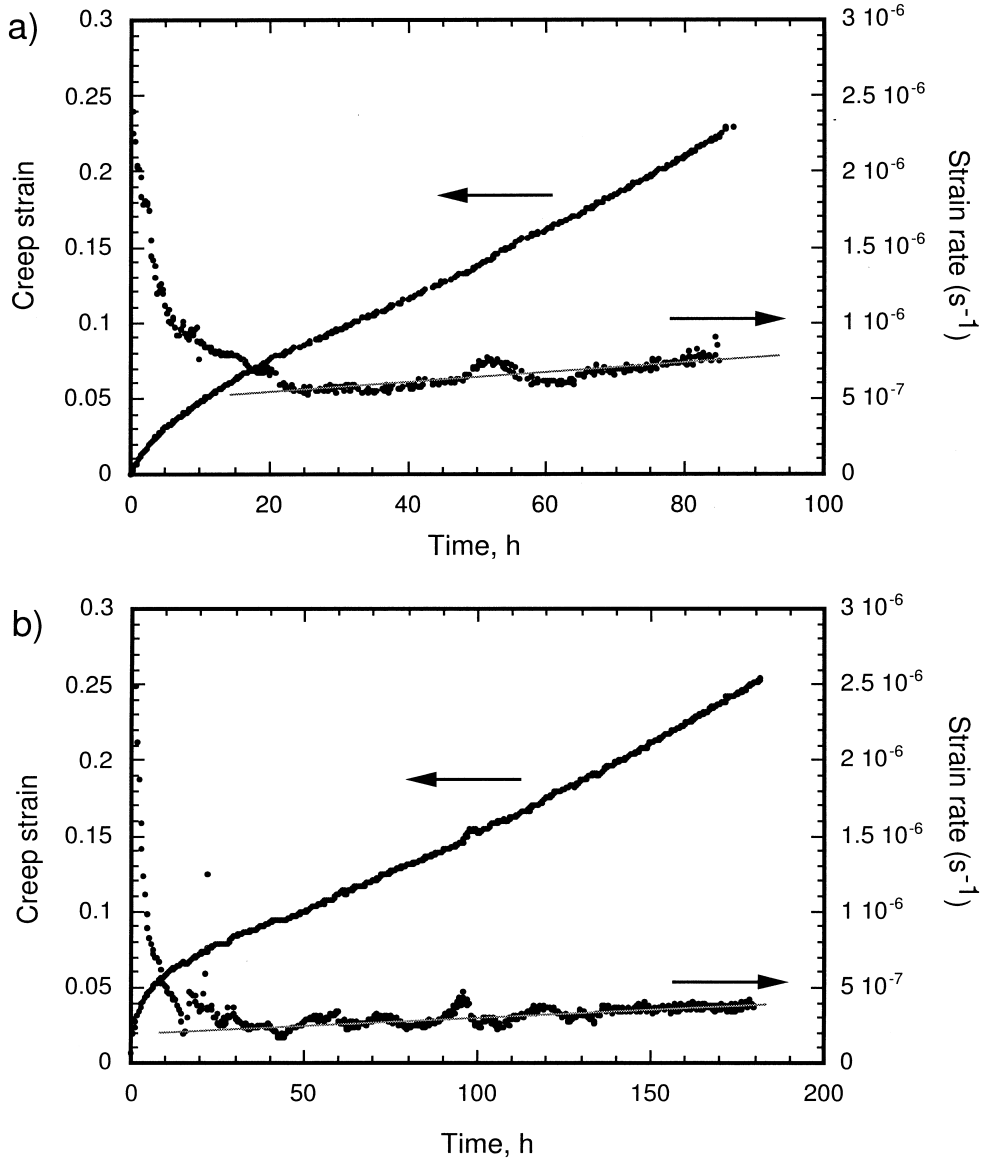

Fig. 3. Creep strains and strain rates of silicon nitride conducted at (a) 1400°C under a stress of 70 MPa, and (b) 1400°C under a stress of 50 MPa.

not been reported.[17–19] Therefore, the gradual increase in the creep rate is attributed to elastic degradation in subsurface layers rather than cavitation damage.

4. Summary

Tensile creep tests of a gas pressure sintered silicon nitride were conducted at elevated temperatures in air. The material contains ytterbium and aluminum in secondary phases and has a typical bimodal grain size distribution. During creep tests, a subsurface intermediate layer was formed between the surface oxidation layer and the core of the material. The effective Young's modulus of the subsurface layer was lower than the core of the specimens and numerous cracks were produced in the intermediate layers. The creep curves exhibit a short transient stage followed by secondary creep, in which the creep rate gradually increases. Such an increase in the creep rate was attributed to the stress increase in the core of the specimen, as a result of a gradual degradation in the elastic modulus and crack generation in the subsurface layers.

Acknowledgements

This work was supported by the New Energy and Industrial Technology Department Organization (NEDO) Project, "Research and Development of Ceramic Gas Turbines (300 kW class)". Support for the stay of one of the authors (F.L.) at JFCC by an STA fellowship is acknowledged. The authors are very grateful for the technical assistance of F. Sakakibara and R. Takebayashi in the elastic modulus measurements.

References

1. Takao, H., Okada, A., Ando, M., Akimune, Y. and Hirosaki, H., Ceramic for reciprocating engines: an application review. In *4th International Symposium on Ceramic Materials and Components for Engines*, ed. R. Carlson, T. Johansson and L. Kahlman. Elsevier Applied Science, London, 1992, pp. 118–133.
2. Matsuda, R., The progress of ceramic parts in engine applications. In *Proceedings of 6th International Symposium on Ceramic Materials and Components for Engines*, ed. K. Niihara, S. Kanzaki, S. Komeya, K. Komeya, S. Hirano and K. Morinaga. Technoplaza Co, Tokyo, Japan, 1998, pp. 274–282.
3. Hattori, M., Yamamoto, T. and Watanabe, K., Development of ceramic gas turbine components for the CGT301 engine. In *Proceedings of 6th International Symposium on Ceramic Materials and Components for Engines*, ed. K. Niihara, S. Kanzaki, K. Komeya, S. Hirano and K. Morinaga. Technoplaza Co, Tokyo, Japan, 1998, pp. 222–227.
4. Nakashima, T., Tatsumi, T., Takehara, I., Ichikawa, Y. and Kobayashi, H., Research and development of CGT302. In *Proceedings of 6th International Symposium on Ceramic Materials and Components for Engines*, ed. K. Niihara, S. Kanzaki, K. Komeya, S. Hirano and K. Morinaga. Technoplaza Co, Tokyo, Japan, 1998, pp. 233–236.
5. Wiederhorn, S. M., Evans, A. G., Fuller, E. R. and Johnson, H., Application of fracture mechanics to space-shuttle windows. *J. Am. Ceram. Soc.*, 1974, **57**, 319–323.
6. Katayama, K., Watanabe, T., Matoba, K. and Katoh, N., Development of Nissan high response ceramic turbocharger rotors. SAE Technical Paper Series, No. 861128. Society of Automobile Engineers, Warrendale, PA, 1986.
7. Quinn, G. D., Fracture mechanism maps for advanced structural ceramics. *J. Mater. Sci.*, 1990, **25**, 4361–4376.
8. Wiederhorn, S. M., Lueche, W. E. and Krause Jr., R. F., A strain-based methodology for high temperature lifetime prediction. *Ceramic Science and Engineering Proceedings*, 1998, **19**, 65–78.
9. Usami, H., Lofaj, F., Okada, A., Ikeda, Y., Mizuta, Y. and Kawamoto, H., Evaluation of creep damage development of quasi-plastic GPS silicon nitride by X-ray computed tomography. In *Engineering Ceramics '96: Higher reliability through Processing*, ed. C. N. Babini, M. Haviar and P. Sajgalih. Kluwer Academic Publishers, Dordrecht, The Netherlands, 1997, pp. 353–362.
10. Lofaj, F., Usami, H., Ikeda, Y., Mizuta Y. and Kawamoto, H., Creep fracture behavior of gas pressure sintered silicon nitride by X-ray CT. In *Proceedings of Yokohama International Gas Turbine Congress Vol. 3*, Gas Turbine Society of Japan, Tokyo, Japan, 1995, pp. 37–44.
11. Lofaj, F., Okada, A., Usami, H., Mizuta, Y., Ikeda, Y. and Kawamoto, H., Quasi-plastic creep deformation in the nano-sized Si_3N_4 composite. In *Proceedings of the International Conference: Fractography '97*, ed. L'. Parilak, Slovakia, 1997, pp. 309–318.
12. Lofaj, F., Okada, A., Usami, H. and Kawamoto, H., Creep damage in an advanced self-reinforced silicon nitride: part 1, cavitation in the amorphous boundary phase. *J. Am. Ceram. Soc.*, 1999, **82**, 1009–1019.
13. Lofaj, F., Okada, A., Usami, H. and Kawamoto, H., Cavitation mechanism during tensile creep of an advanced silicon nitride. In *Ceramic Transactions Vol. 71. Mass and Charge Transport in Ceramics*, ed. K. Koumoto, H. Matsubara and L. Sheppard. American Ceramic Society, Westerville, OH, 1996, pp. 585–599.
14. Lofaj, F., Usami, H., Okada, A. and Kawamoto, H., Long-term creep damage development in a self-reinforced silicon nitride. In *Engineering ceramics '96: Higher Reliability through Processing*, ed. G. N. Babini, M. Haviar and P. Sajgalih. Kluwer Academic Publishers, Dordrecht, The Netherlands, 1997, pp. 337–352.
15. Lofaj, F., Cao, J.-W., Okada, A. and Kawamoto, H., Comparison of creep behavior and creep damage mechanisms in the high-performance silicon nitrides. In *Proceedings of 6th International Symposium on Ceramic Materials and Components for Engines*, ed. K. Kanzaki, S. Kanzaki, K. Komeya, S. Hirano and K. Morinaga. Technoplaza Co, Tokyo, Japan, 1998, pp. 713–718.
16. Lofaj, F., Okada, A. and Kawamoto, H., Cavitational strain contribution to tensile creep in vitreous bonded ceramics. *J. Am. Ceram. Soc.*, 1997, **80**, 1619–1623.
17. Menon, M. N., Fang, H. T., Wu, D. C., Jenkins, M. J. and Ferber, M. K., Creep and stress rupture behavior of an advanced silicon nitride: part II, creep rate behavior. *J Am. Ceram. Soc.*, 1994, **77**, 1228–1234.
18. Wiederhorn, S. M., Roberts, D. E., Chuang, T. J. and Chuck, L., Damage-enhanced creep in a siliconized silicon carbide: phenomenology. *J. Am. Ceram. Soc.*, 1988, **71**, 602–608.
19. Ohji, T. and Yamauchi, Y., Diffusional crack growth and creep rupture of silicon carbide doped alumina. *J Am. Ceram. Soc.*, 1994, **77**, 678–682.